



AN INTERDISCIPLINARY APPROACH FOR REGIONAL SEISMIC DAMAGE ESTIMATION

A. Askan⁽¹⁾, A. Erberik⁽²⁾, S. Karimzadeh⁽³⁾, A. Yakut⁽⁴⁾, F. N. Sisman⁽⁵⁾, N. Kilic⁽⁶⁾, M. Asten⁽⁷⁾

⁽¹⁾ Assoc. Prof., Middle East Technical University, aaskan@metu.edu.tr

⁽²⁾ Prof., Middle East Technical University, altug@metu.edu.tr

⁽³⁾ Postdoctoral researcher, Middle East Technical University, sh_naghshineh@yahoo.com

⁽⁴⁾ Prof., Middle East Technical University, ayakut@metu.edu.tr

⁽⁵⁾ Position, Middle East Technical University, f.nurtensisman@gmail.com

⁽⁶⁾ PhD, Earthquake Department, Prime Ministry Disaster and Emergency Management Authority, Ankara, Turkey, nazan.yilmaz@afad.gov.tr

⁽⁷⁾ Prof., Monash University, michael.asten@monash.edu

Abstract

In order to mitigate seismic risk in urban regions, the first task is to identify potential seismic losses in future earthquakes. Seismic loss estimation is an interdisciplinary framework including a wide range of contributions from geophysical and earthquake engineers, physical and economic planners to insurance companies. In this study, a moderate size city in Turkey, namely Erzincan, is modeled completely from geophysical attributes to the built environment. Erzincan city is on the eastern part of the North Anatolian Fault zone and it is located in the close vicinity of a triple conjunction of major fault systems within a basin structure. The city experienced two major events in the twentieth century; $M_s \approx 8.0$ in 1939 and $M_w = 6.6$ in 1992. Hence as a study area, the city under concern has significant hazard potential. The main components of the study are probabilistic and deterministic seismic hazard assessment and estimation of potential ground motions, regional building fragility information for residential buildings and damage estimation by using the generated fragility functions. The initial results are in terms of key components such as construction of soil profiles, ground motion simulations of past earthquakes and scenario events, site-specific probabilistic seismic hazard analyses and fragility functions derived using regional building characteristics along with simulated regional ground motion data. The proposed approach is examined by comparing the observed damage and the estimated damage for the 1992 event, for which the results seem to have a reasonable match in between. After verification, the seismic damage distribution in the city for scenario event of $M_w = 7$ is hypothetically calculated as a case study for potential damage prediction. The estimated damage levels in the city center reveals that Erzincan is under significant seismic threat due to its close distance from the fault system in the North, soft soil conditions within Erzincan basin as well as the seismic vulnerability of the building stock in the region. Finally, a brief discussion on the applicability of EMS-98 building types, vulnerability classes and damage grades to the proposed methodology is presented.

Keywords: site characterization; probabilistic seismic hazard analysis; ground motion simulation; vulnerability; damage

1. Introduction

Seismic risk mitigation is crucial in urban regions with significant seismic hazard. For mitigation and management of risk in such regions, seismic damage and loss estimations are carried out. The fundamental components of any damage estimation algorithm are seismic hazard with reliable soil information, building vulnerability and damage calculations. The accuracy of damage estimations depends on the quality of the input data and physical modeling of the involved processes.

This study presents an integrated damage estimation framework that was developed within a national project led by an interdisciplinary team consisting of geological, geophysical and civil engineers. An application of the proposed method in terms of city-level damage estimation is also provided. The key aspect of the method is the fact that all components are modeled using regional properties in detail. The main component of the method is the estimation of the local soil properties in the study area. For this purpose, the first step involves passive seismic methods on microtremor measurements in the field. As a result, one-dimensional S-wave velocity models are derived at selected nodes. The second step includes probabilistic and deterministic seismic hazard analyses. Probabilistic analyses consider the activities of each regional source within a probabilistic framework. Deterministic analyses involve simulation of ground motions and construction of a synthetic regional ground motion dataset. Next, building fragility models are derived considering the regional characteristics of the building stock. Finally, damage distributions are estimated for the study area using the derived fragilities and the synthetic ground motion database. In order to verify the proposed approach, damage estimations are performed for a past earthquake in the region; then predictions are presented for a potential large event. In this paper, the main aspects of the components and the fundamental results obtained within the mentioned project will be presented. Further details regarding the data, models and the applications can be found in Askan *et al.* [1, 2].

The study area is the Erzinçan city center in Eastern Turkey. The city is located at the intersection of three active fault zones: North Anatolian Fault Zone (NAFZ), North East Anatolian Fault Zone (NEAFZ) and Ovacık Fault. The area is considered to be one of the most hazardous regions of the world. Historical records evidence 18 large ($M > 8$) earthquakes in the close vicinity of Erzinçan within the past 1000 years [2]. NAFZ displays right-lateral strike-slip faulting whereas East Anatolian Fault Zone (EAFZ) and NEAFZ have left-lateral strike-slip faulting. The city center is built on an alluvium pull-apart basin with dimensions of 50 km x 15 km.

In the last century, Erzinçan experienced two destructive earthquakes: The first one was the 1939 earthquake ($M_s \sim 8.0$) that caused severe structural damage leading to more than 30,000 fatalities. The second was the 1992 earthquake ($M_w = 6.6$) that led to major structural damage in the city center resulting in major structural and economic loss and approximately 500 fatalities (e.g.: [3]). The epicenters of these earthquakes as well as the corresponding faults and source mechanisms are displayed in Fig. 1.

2. Site Characterization: Construction of S-wave Velocity Models

Recently, due to the cost and feasibility issues of active methods in urban regions, alternative methods have been developed including the non-invasive seismic methods. In this study, a passive seismic approach which relies on analyses of microtremors is employed to estimate the 1-D wave velocity profiles: a development of the original Spatial Autocorrelation (SPAC) method ([4-6]) to include higher-mode effects is used herein. This latter approach is named MMSPAC which is described extensively in Asten [7]. The fundamental objective of this approach is to estimate the S-wave velocity structure by analyzing the coherencies of the measured microtremor wave fields.

The traditional SPAC method employs circular arrays. However, MMSPAC method is shown to be effective in other configurations such as the triangular arrays even in the existence of highly directional energy with sufficiently close azimuthal sampling (e.g.: [7, 8]).

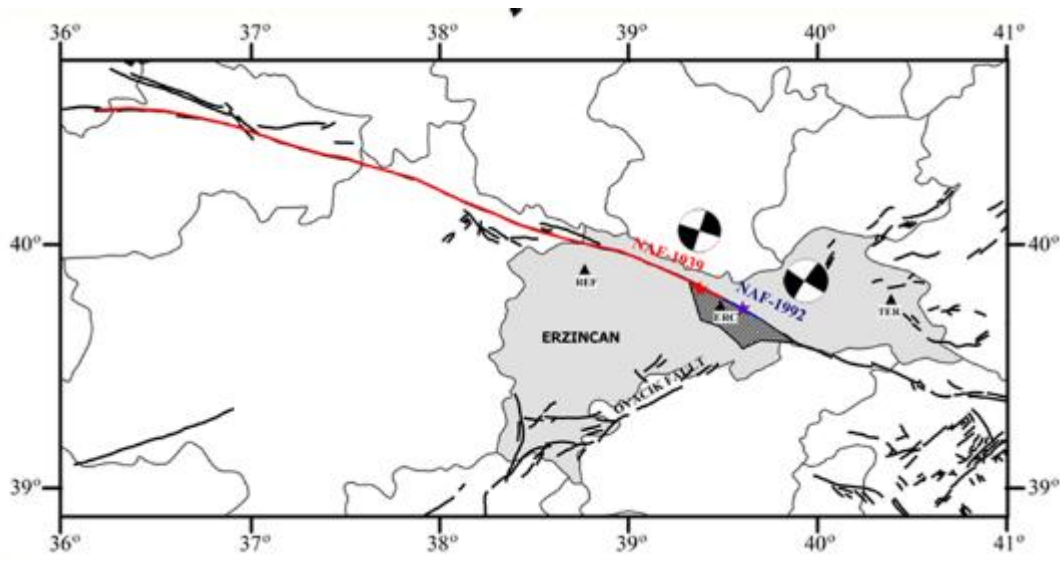


Fig. 1 – Map showing the rupture zones, mechanisms and epicenters of the 1939 and 1992 Erzincan earthquakes (indicated with red and blue colors, respectively) and strong ground motion stations that recorded 1992 Erzincan earthquake (indicated with black triangles). Erzincan basin is also shown within a shaded polygon parallel to the 1992 fault. (Fig. 1 is adapted from Askan et al. [9])

The direct fitting of modeled and observed SPAC spectra relies on the following relationship between coherency and phase velocity:

$$C_m(f) = J_0\left(\frac{2\pi f r}{v_p(f)}\right) \quad (1)$$

where $C_m(f)$ is the modeled spatially-averaged coherency, f is frequency, J_0 is the Bessel function of the first type and zero-order, r is the station separation, and $v_p(f)$ is the modeled phase velocity for a layered earth.

The process of direct fitting of observed and modeled SPAC removes the need for an intermediate step of computing observed phase velocities which is a nonlinear and non-unique problem. The direct fitting is achieved by iterative forward modeling; the quality of the fit over a selected bandwidth is measured by the root-mean-square error between the observed and modeled SPAC. Further details of the methodology and microtremor dataset can be found in [1].

In this study, MMSPAC analyses are performed on microtremor data collected at 9 selected sites within Erzincan city center (Fig. 2). Subsequent inclusion of Horizontal-to-Vertical Spectral Ratios (HVSR) as outlined by Nakamura [10] in the curve fitting process extends useful frequencies up to a decade lower than those for MMSPAC alone as shown in Askan et al. [1]. Thus, addition of HVSR information in the MMSPAC modeling helps to estimate the bedrock depth and the corresponding V_s levels in bedrock. The 1-D wave velocity profiles obtained at the selected nodes are presented in Fig. 3, which is constructed such that each of the panels displays 3 sites grouped together in order to observe the basin structure in the NS and EW directions. It is observed that the northern regions (Sites 2 and 8) are quite stiff while the southern areas near the Erzincan Airport (Site 1) are located on softer soil deposits. The basin structure is also noticeable when the velocity profiles along the North-South and East-West directions are compared.

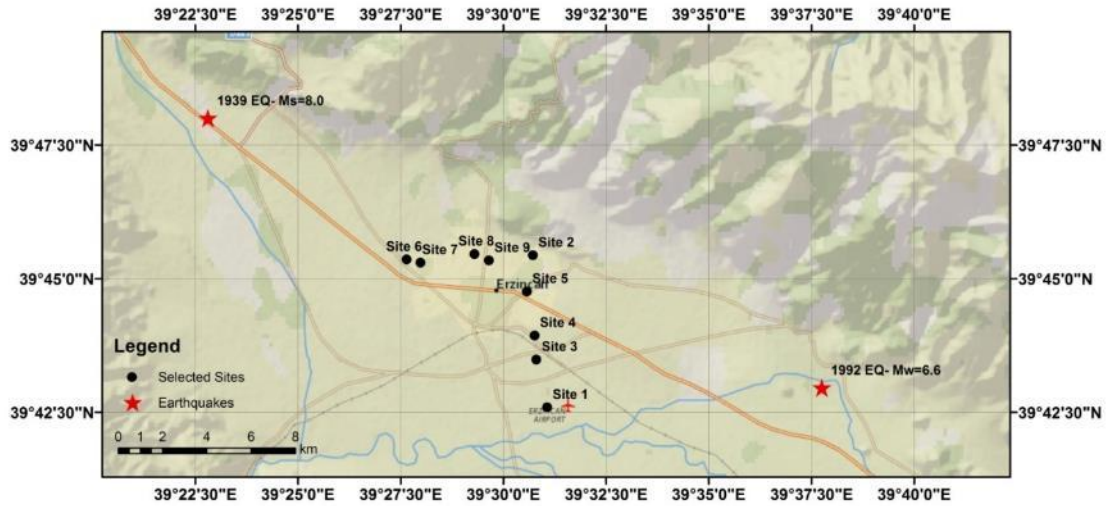


Fig. 2 – Location of the selected sites for MMSPAC analyses in Erzincan basin

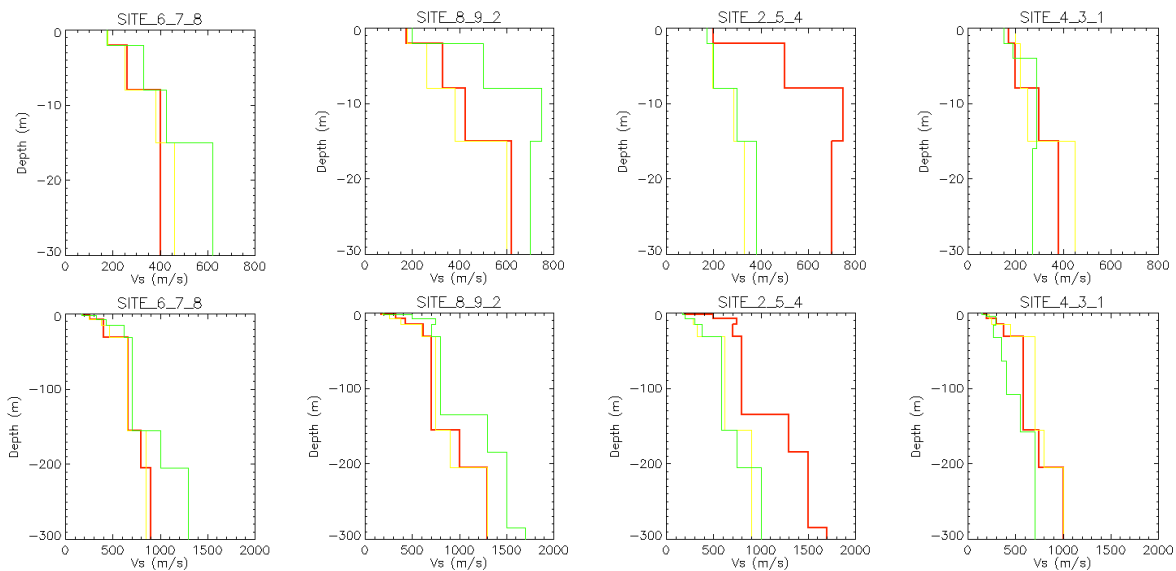


Fig. 3 – 1D velocity and models for the first 30m (top panels) and 300m (bottom panels) at the selected sites (For each panel, the models at sites with ascending numbers are indicated with red, yellow and green colors, respectively)

Finally, it is well known that the local soil conditions significantly affect the amplitude and frequency content of the ground motions. It must be noted that within the damage estimation framework proposed herein, the velocity models presented in Fig. 3 are used as important input parameters in the seismic hazard analyses as follows: In probabilistic seismic hazard analyses Vs30 values are employed while in ground motion simulations the soil models are used to compute soil amplification factors in the frequency domain.

3. Seismic Hazard Analyses

In this stage of the proposed method, the information on the active faults in the study region and the local soil models are used to perform both probabilistic and deterministic seismic hazard analyses. The related methods and results will be briefly summarized herein. Further details can be found in [1].

3.1 Probabilistic Seismic Hazard Analyses (PSHA)

The classical PSHA model was originally developed by Cornell [11] in order to compute and express the seismic hazard of a region within a probabilistic framework. The fundamental steps of probabilistic seismic hazard analyses can be as follows: Identifying the seismic sources that remain within a region of interest; modeling a magnitude-frequency relationship for each source in the region; constructing a model for the temporal occurrence of the earthquakes; selecting a ground motion parameter of interest to indicate the seismic hazard; choosing or forming a model that determines the attenuation of this parameter with distance; and lastly estimating the probabilities of exceeding different levels of the selected ground motion parameter by aggregating the contributions of all seismic sources in the region of interest.

In this study, while performing PSHA analyses for Erzincan city center, initially the regional catalog and seismic sources are studied in detail. Then the local soil models are taken from the previous step in the form of V_{s30} values at selected nodes. Finally, regional ground motion prediction equations are employed in the analyses to reflect the regional seismic characteristics. A total of 123 nodes are selected within Erzincan city center for PSHA analyses and probability distributions of selected ground motion parameters such as peak ground acceleration (PGA) and spectral acceleration are obtained. In the analyses, at every node, the V_{s30} value of the closest node with an available soil profile is adopted.

Fig. 4 demonstrates the results of PSHA analyses in the form of seismic hazard maps for different return periods in terms of PGA. The results indicate the significant seismic hazard in Erzincan region. It must be noted that the hazard maps in terms of spectral accelerations yield similar results.

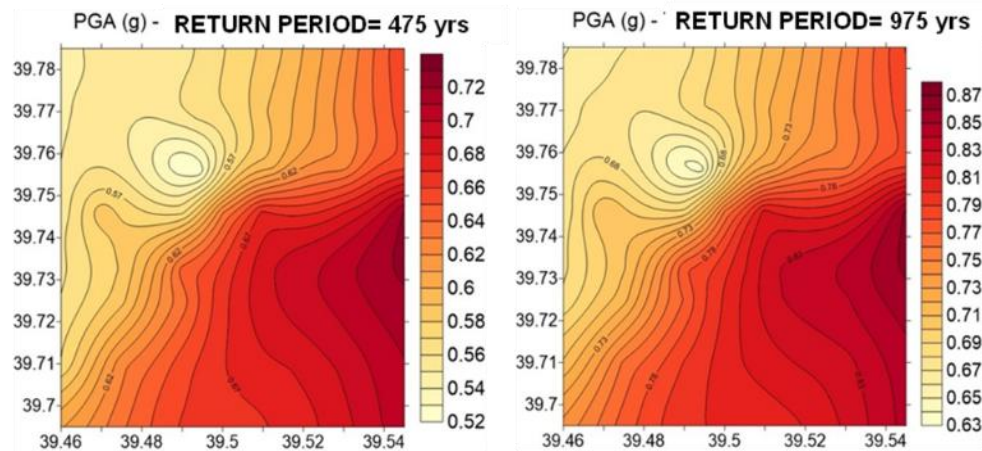


Fig. 4 – Probabilistic seismic hazard maps in Erzincan in terms of PGA for different return periods using the local soil profiles presented in the previous section

3.2 Deterministic Seismic Hazard Analyses (DSHA): Ground Motion Simulations of Scenario Events

In some cases, hazard analyses are required to assess the seismic hazard of a region under specific earthquake scenarios. In such cases, DSHA are employed to obtain the potential ground motion time histories of a scenario event (or in some cases of a past earthquake). In this study, stochastic finite-fault simulation methodology as outlined in Motazedian and Atkinson [12] is employed.

In this method, ground motions are assumed to radiate from a rectangular finite-fault divided into subfaults, each of which is modeled as a stochastic point source with an w^{-2} spectrum. The stochastic point source model relies on a deterministic target spectrum that is expressed as a multiplication of source, path and site filters ([13]). In the finite-fault model, the hypocenter of the earthquake is taken to be on one of the subfaults, and the rupture propagates radially from the hypocenter. Each subfault is triggered when the rupture reaches the center of that subfault. The contribution of all subfaults is summed with appropriate time delays in order to obtain the entire contribution of the fault plane to the seismic field, at any observation point. In the dynamic corner frequency approach developed by Motazedian and Atkinson [12], the total energy radiated from the fault is conserved regardless of the selected subfault size. In this study, the dynamic corner frequency approach as implemented in the computer program EXSIM ([12]) is employed.

In this study, to verify the source, path and site parameters used in the simulations, initially the 1992 ($M_w=6.6$) Erzincan earthquake is simulated. The comparisons of observed and simulated waveforms at the recording stations indicate that the input parameters can be employed in regional ground motion simulations ([9]). Then, simulations are performed for a set of scenario events in Erzincan city center with magnitudes of $M_w=5.0$, $M_w=5.5$, $M_w=6.0$, $M_w=6.5$, $M_w=7.0$ and $M_w=7.5$ on the same fault that caused the 1992 Erzincan earthquake. Since the epicenter of that event (Fig.1) is critical in terms of distance from the city center, the epicenter of the scenario events is assumed to be at the same location. For each scenario earthquake, the full waveforms are obtained at 123 nodes in the city center as mentioned in the previous section. A synthetic ground motion database is formed that contains the simulated waveforms at each node for each event. Due to space reasons, rather than presenting the waveforms herein, the spatial distribution of simulated peak ground acceleration and spectral acceleration (SA) values at different periods are demonstrated from a selected scenario event ($M_w=7.0$) in Fig. 5.

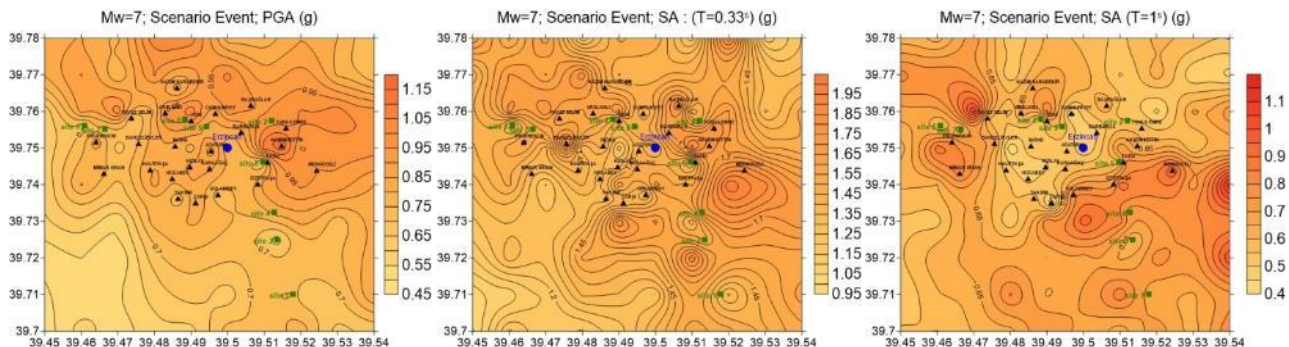


Fig. 5 – The spatial distribution of simulated ground motions in Erzincan due to a scenario event of $M_w=7.0$

Fig. 5 indicates that for the scenario earthquake with $M_w = 7.0$, the city center experiences significantly high PGA as well as spectral acceleration levels (exceeding $1g$ at several locations). As stated previously, the city center is located on a basin of deep soft soil deposits. The soils are softer in the southern region, resulting in the large amplitudes in the south. There are relatively stiffer sites in the northern region; however, the fault plane is close to those nodes located in the north, which results in overall higher amplitudes at these locations as well. These observations coupled with the building vulnerability in the region explain the severity of the observed damage during the 1992 event and point to the significant seismic risk in Erzincan area. We note that ground deformations such as liquefaction are not modeled in this study. Thus, effects of these phenomena on structural damage are not considered herein.

The simulated waveforms for the mentioned scenario events with $M_w=5.0-7.5$ are used in the derivation the regional fragility curves as explained in the following sections.

4. Seismic Fragility of Building Models

This phase of the study is focused on estimating the damage state probabilities of different structural building classes in the study region on the district level by using fragility curves. In order to achieve this task, a site survey was conducted in the Erzincan city to identify and classify the local construction types and their inherent structural characteristics. Based on the results of this site survey in the city center of Erzincan, the residential building stock was classified into 21 groups in accordance with three parameters: type of construction, number of stories and level of compliance with seismic design principles. Hence, there exist 12 RC (frame, shear wall or dual type) and 9 masonry building sub-classes. Next, the local and specific structural characteristics of the existing building classes in the region were idealized by using equivalent single degree of freedom (ESDOF) models. The final step was to construct the fragility curve sets of the considered building classes through dynamic analyses of the simplified ESDOF models subjected to a selected set of synthetic ground motion records. These records have been generated by the methodology explained in the previous section.

In order to simulate the inherent cyclic characteristics of each building sub-class under earthquake excitations and to obtain the response statistics of ESDOF models through nonlinear time-history analyses (NLTHA), a multi-parameter hysteresis model, named as “Modified Ibarra–Medina-Krawinker Deterioration Model” [14], was selected. This hysteresis model, which had been embedded into the OpenSees analysis platform [15], is a peak-oriented deterioration model (Fig. 6). It is able to simulate various modes of cyclic deterioration in strength and stiffness such as basic strength, post-capping strength, unloading stiffness, and reloading stiffness deterioration that may be observed in the real inelastic behavior.

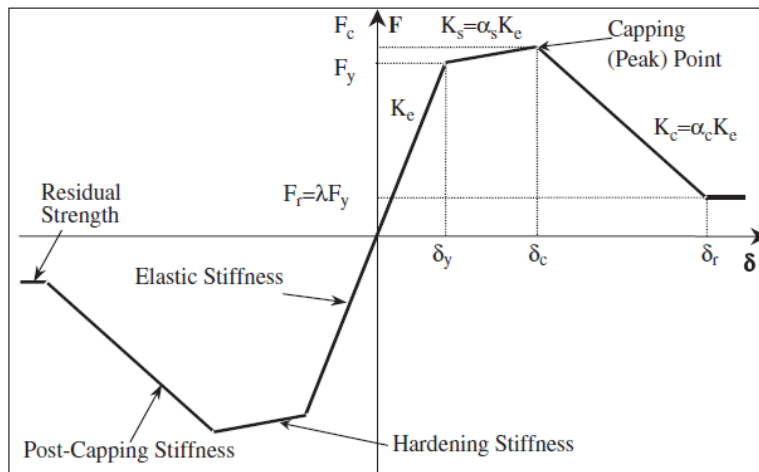


Fig. 6 – Backbone curve for hysteresis model (adopted from Ibarra *et al.* [14])

The major response parameters of the ESDOF models, which are period (T), strength ratio (η) and ductility factor (μ), are considered as random variables in this study. For sampling of the random variables, Latin Hypercube Sampling (LHS) method [16] was selected and 20 samples were generated for each random variable. This sample size had been proved to be adequate in order to quantify the structural variability in seismic fragility analysis of similar types of building structures [17]. Other hysteresis model parameters were assumed to be constant for the simulations in each building sub-class. Then the generated building simulations were analyzed under a specific set of synthetic ground motion records by using nonlinear time history analyses to obtain the response statistics. The schematic flow of the applied fragility analysis approach is shown in Fig. 7. The process starts by the construction of response statistics (in terms of maximum displacement of ESDOF system, denoted as “D”) as a function of the selected ground motion intensity parameter (in this study, it is selected as peak ground velocity, PGV, for RC structures and peak ground acceleration, PGA, for masonry structures). This is in accordance with the previous studies stating that PGV and PGA correlate well with inelastic response of flexible

structures (RC frame) and stiffer structures (masonry), respectively [17, 18]. The horizontal line labeled as LS_i represents the specified limit (or performance) state (Fig. 7.a). In this study, three performance levels are considered as Immediate Occupancy (LS_1), Life Safety (LS_2) and Collapse Prevention (LS_3). For the scattered data of the j^{th} ground motion intensity level, GMI_j (see Fig. 7.b), the conditional probability of attainment or exceedance of the i^{th} limit state (LS_i) at the j^{th} ground motion intensity level is calculated by using the following formula:

$$P(D \geq LS_i | GMI_j) = n_A / n_T \quad (2)$$

where n_A is the sum of responses equal or above the i^{th} limit state, and n_T stands for the total number of responses at the j^{th} ground motion intensity level. After repeating this process for different intensity levels, the discrete fragility information presented in Fig. 7.c can be obtained for a certain limit state. A cumulative lognormal distribution function is fitted to the obtained data with least squares technique as illustrated in Fig. 7.d. To derive fragility curves for all building types, this process is repeated for three limit states and all 21 sub-classes. In this paper, it is not possible to present all the fragility curve sets due to space limitations. Therefore, only a representative set of curves are given in Fig. 8 for the purpose of demonstration.

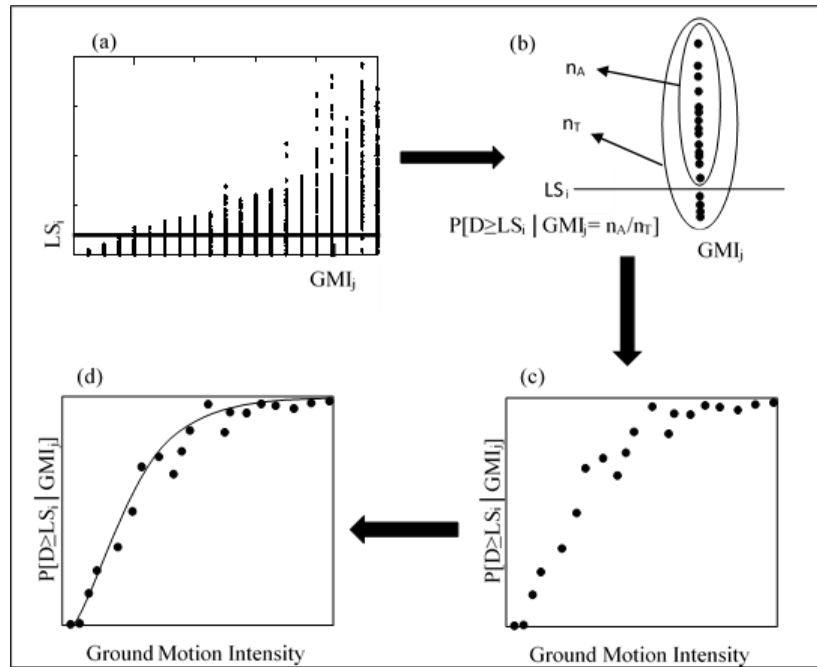


Fig. 7 – Schematic representation of the fragility curve generation procedure

5. Regional Damage Estimation Methodology

The steps of the regional damage estimation methodology proposed in this study can be defined as follows:

- Scenario earthquake is identified.
- Distribution of the considered ground motion intensity parameter (PGA or PGV) throughout the study region is obtained by using the database of synthetic ground motion records.
- The building sub-classes and their percentage in the study region are determined.
- Damage ratios (DR) and central damage ratios (CDR) of the existing building sub-classes in the region are calculated by using the generated fragility curves.
- A single mean damage ratio (MDR) is calculated for each building sub-class by using the damage state probabilities and the CDRs.
- Finally, an overall MDR is calculated for each residential area by considering the percent distributions of building sub-classes in the region.

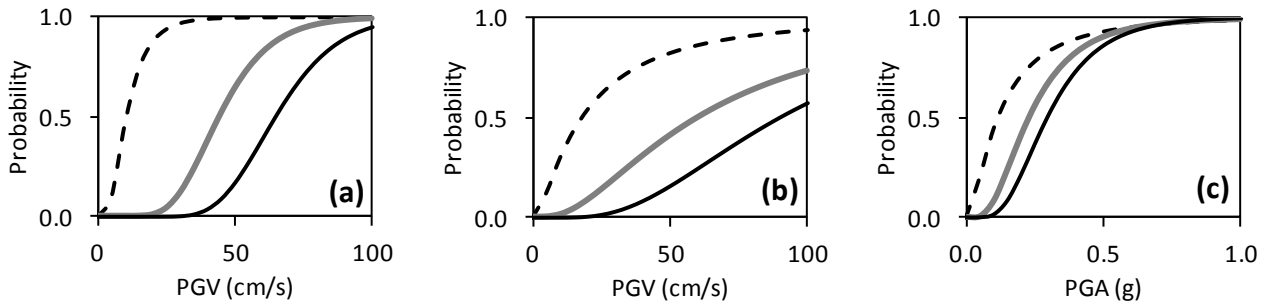


Fig. 8 – Fragility curves for (a) mid-rise RC frame buildings, (b) mid-rise RC dual buildings, (c) 2 story URM buildings where the dashed lines correspond to LS_1 , the gray solid lines to LS_2 , and the black solid lines to LS_3

First, the verification of the proposed regional damage estimation methodology is done for the 1992 Erzincan Turkey earthquake ($M_w=6.6$) by comparing the estimated damage distribution in the city that was obtained by the methodology and the observed damage distribution just after the earthquake in terms of MDR values. The results are presented in Fig. 9. In the verification analysis, the selected districts are the ones for which the characteristics of the building stock are known. In the plots, the legend “N/A Data” means in the related districts, there exists no building information, therefore MDR value cannot be calculated. Comparing the estimated and observed damage distributions in Fig. 9 it can be stated that mean damage for a significant percentage of the residential districts is in close agreement for the 1992 earthquake scenario. For the rest of the districts, it is observed that the estimated damage distribution is more severe than the actual one. These districts are generally the ones that are close to the fault, which created the 1992 event. The reason of this discrepancy may be attributed to the subjectivity and bias in collecting the damaged building data during post-earthquake field observations and also to the assumptions and simplifications of the proposed damage estimation model (selection of ground motion simulation parameters, use of simplified ESDOF models, etc.) But overall, the proposed model is deemed to be eligible for regional damage estimation studies in Erzincan city for different scenario earthquakes.

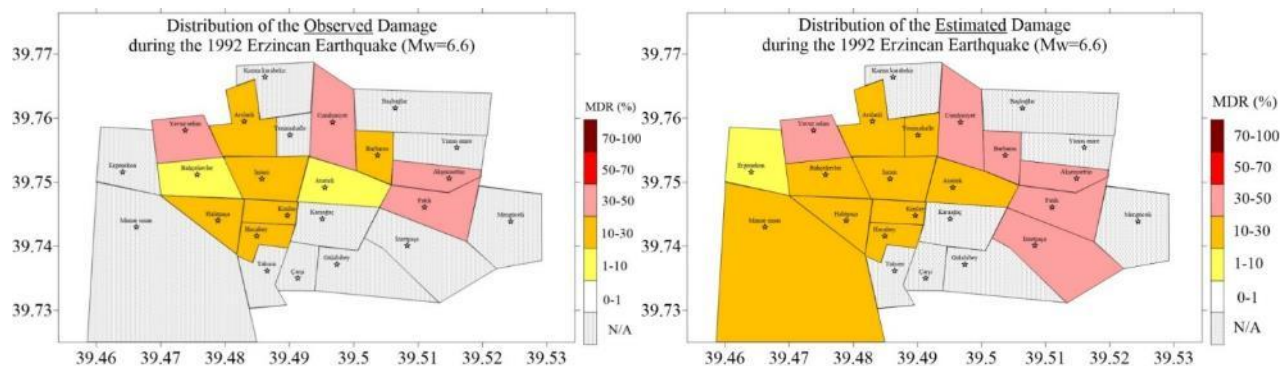


Fig. 9 – Distribution of the (a) observed and (b) estimated MDRs in the Erzincan region for the 1992 Erzincan earthquake

Then, as a seismic damage estimation exercise, damage distribution of the considered residential districts in Erzincan city is estimated for a scenario event with $M_w=7.0$. The resulting damage distribution is shown in Fig. 10. While interpreting these results, it should be noted that the epicenter of the scenario earthquake is chosen in such a way that it will cause the most severe effect in terms of location and distance. According to the estimated damage distribution, 6 out of 16 districts experience severe damage with MDR values between 50% and 100%. The remaining districts seem to experience moderate damage with MDR values between 10% and 50%. Hence it can be concluded that Erzincan city center is under high seismic risk in the case of a major earthquake (order of magnitude 7) both from regional seismic activity and building stock fragility points of view.

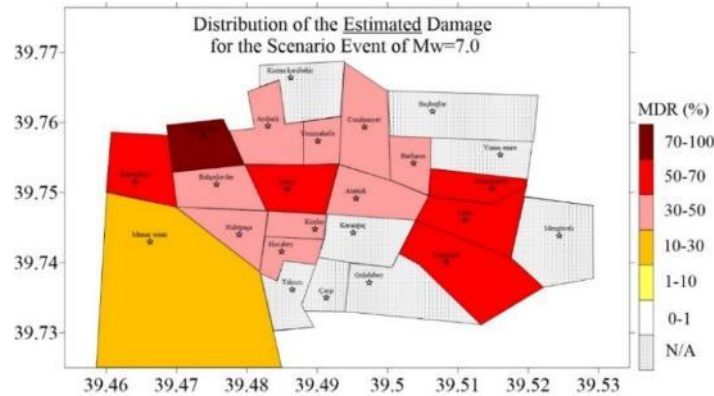


Fig. 10 – Distribution of the estimated MDRs in the Erzincan region for scenario event of $M_w=7.0$

6. Applicability of EMS-98 to the Proposed Methodology

European Macroseismic Scale, EMS-98 [19] is not only a simple seismic intensity scale but it also includes building types and vulnerability classes to assess seismic vulnerability of structures in terms of qualitative damage grades in a practical and manageable way. This section briefly discusses the applicability of EMS-98 building types, vulnerability classes and damage grades to the methodology developed in this study.

In the EMS-98 methodology, masonry buildings are classified as rubble stone/field stone, simple stone, massive stone, adobe, unreinforced (with manufactured stone units or with RC floors) and reinforced/confined. This classification is different from the one that has been used in this study due to the fact that local construction practices are quite different in the study region. The nine sub-classes of masonry buildings considered are all unreinforced masonry independent of wall material type. Previous post-earthquake observations have revealed that number of stories is an important parameter for seismic performance of Turkish masonry buildings, hence it is considered from one to three stories. For RC buildings, classification in EMS-98 include frame and wall buildings with high and moderate levels of earthquake resistant design (ERD) in addition to frame and wall buildings without ERD. In this study, only RC frame building classes have been considered since RC wall buildings constitute a small percentage in the overall building stock of the study region. Again, number of stories is considered as a major parameter where RC frame buildings are classified as low-rise (1-3 stories) and midrise (4-8 stories).

Another classification in EMS-98 is the vulnerability class. There exist six classes of decreasing vulnerability from A to F. A similar sub-classification also exists in this study by the help of a parameter related to the level of compliance with seismic design codes and construction principles. There are three levels from low to high, which can be somehow linked to seismic resistance to earthquake generated shaking (i.e. vulnerability). By comparing the definitions, it is appropriate to assign vulnerability classes A, B and C to masonry buildings in this study whereas for RC frame buildings, vulnerability classes C, D & E seem to be consistent with the proposed classification in terms of the level of code compliance.

For damage grades, the EMS-98 methodology defines five grades from none/slight damage to collapse for both masonry and RC buildings in a qualitative manner. On the other hand, in this study, seismic damage is estimated by comparing seismic demand obtained from nonlinear dynamic analyses to structural capacity defined in terms of limit states in quantitative manner. The three limit states in this study can be matched with the five damage grades in EMS-98 in a rough manner. Accordingly, these limit states can be assumed to be close to the qualitative definitions of grades 1, 3 and 5, respectively.

Overall, the proposed approach and the EMS-98 methodology have major differences in spite of their common points. The differences generally arise from the specific and local data used for the study region and different characteristics of these two methods (i.e. qualitative versus quantitative approach).

7. Conclusions

The ground motion intensity and seismic damage distribution maps in Erzincan city reveal that there is a significant seismic threat due to the close distance to the active faults and soft soil conditions in the basin where the city resides in addition to a remarkable seismic risk due to the fragility of existing building stock in the area. Although seismic risk assessment studies in Turkey have been focused on the more industrialized and populated west Anatolian part, urgent strategies should be developed also for Erzincan regarding earthquake preparedness and seismic risk mitigation.

In most of the damage estimation studies in the literature, some of the ingredients (i.e. soil characteristics, ground motion, building information and its vulnerability, etc.) are obtained without local data and detailed analysis or they are directly adapted from other similar studies. The novelty of the proposed damage estimation methodology in this study comes from the fact that all the ingredients starting from the seismic source up to the fragility of the infrastructure have been derived in an interdisciplinary manner by using local parameters and by considering the fundamental principles of engineering seismology and earthquake engineering. It is possible to use this integrated methodology for other regions in Turkey or any earthquake prone region in the world. In the long term, the results obtained from such seismic damage estimation studies can be used in practice provided that an active cooperation between academic research units and local authorities is established. Comparing the proposed method with the EMS-98 methodology, it is observed there are major differences, which generally arise from the use of specific and detailed local parameters for the study region.

8. References

- [1] Askan A, Karimzadeh S, Asten M, Kilic N, Sisman FN, Erkmén C (2015a): Assessment of seismic hazard in the Erzincan (Turkey) region: construction of local velocity models and evaluation of potential ground motions. *Turkish Journal of Earth Sciences*, **24** (6), 529-565.
- [2] Askan A, Karimzadeh S, Asten M, Kilic N, Sisman FN, Erkmén C (2015b): Estimation of Potential Seismic Damage in Erzincan, *Technical Report TUJJB 2015/04*, Turkish Union of National Geodesy and Geophysics (TUNGG), Ankara, Turkey (in Turkish).
- [3] Akinci A, Malagnini L, Herrmann RB, Pino NA, Scognamiglio L, Eyidogan H (2001): High-frequency ground motion in the Erzincan region, Turkey: Inferences from small earthquakes. *Bulletin of Seismological Society of America* **91**, 1446–1455.
- [4] Aki K (1957): Space and time spectra of stationary stochastic waves, with special reference to microtremors. *Bulletin of the Earthquake Research Institute of Tokyo University* **35**, 415–456.
- [5] Toksöz MN (1964): Microseisms and an attempted application to exploration. *Geophysics* **29:2**, 154-177.
- [6] Okada H (2003): The Microtremor Survey Method. *Geophysical Monograph Series* **12**, SEG, Tulsa.
- [7] Asten M (2006): On bias and noise in passive seismic data from finite circular array data processed using SPAC methods. *Geophysics* **71**, V153– V162.
- [8] Asten MW, Askan A, Ekincioglu EE, Sisman FN, Uğurhan B (2014): Site characterization in northwestern Turkey based on SPAC and HVSR analysis of microtremor noise. *Exploration Geophysics* **45**: 74–85.

- [9] Askan A, Sisman FN, Ugurhan B (2013): Stochastic strong ground motion simulations in sparsely monitored regions: A validation and sensitivity study on the 13 March 1992 Erzincan (Turkey) earthquake. *Soil Dynamics and Earthquake Engineering*, **55**, 170-181.
- [10] Nakamura Y (1989): A method for dynamic characteristics estimation of subsurface using microtremor on the ground surface, *Quarterly Report of the Railway Technology Research Institute*, **30**, 25–30, Japan.
- [11] Cornell CA (1968): Engineering Seismic Risk Analysis. *Bulletin of the Seismological Society of America* **58:5**, 1583-1606.
- [12] Motazedian D, Atkinson GM (2005): Stochastic finite-fault modeling based on a dynamic corner frequency. *Bulletin of Seismological Society of America* **95**, 995–1010.
- [13] Boore DM (1983): Stochastic simulation of high-frequency ground motions based on seismological models of the radiated spectra. *Bulletin of Seismological Society of America* **73**, 1865–1894.
- [14] Ibarra LF, Medina RA, Krawinkler H (2005): Hysteretic models that incorporate strength and stiffness deterioration. *Earthquake Engineering and Structural Dynamics*, **34** (12), 1489–1511.
- [15] OpenSees 2.4.5. Computer Software, University of California, Berkeley, CA. Retrieved from <http://opensees.berkeley.edu>.
- [16] McKay MD, Conover WJ, Beckman RJ (1979): A comparison of three methods for selecting values of input variables in the analysis of output from a computer code. *Technometrics* **221**, 239–245.
- [17] Erberik MA (2008a): Fragility-based assessment of typical mid-rise and low-rise RC buildings in Turkey. *Engineering Structures*, **30** (5), 1360-1374.
- [18] Erberik MA (2008b). Generation of fragility curves for Turkish masonry buildings considering in-plane failure modes. *Earthquake Engineering and Structural Dynamics* **37** (3), 387-405.
- [19] Grünthal G, Musson R, Schwarz J, Stucchi M (1998): European Macroseismic Scale 1998, Cahiers de Centre Européen de Géodynamique et de Seismologie, Volume 15, Luxembourg.